

# Inhibitory Effects of B-, C-, and E-Ring-Truncated Deguelin Derivatives Against A549, HCT116, and MCF-7 Cancer Cells

John Alfon P. Francisco and Monissa C. Paderes\*

Cite This: *ACS Omega* 2023, 8, 43109–43117

Read Online

ACCESS |



Metrics &amp; More

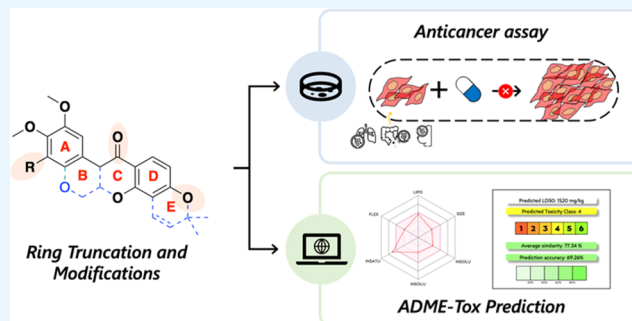


Article Recommendations



Supporting Information

**ABSTRACT:** Deguelin has been extensively studied for its anticancer properties; however, its clinical application has been hindered by concerns about *in vivo* toxicity. Structural modifications of deguelin including ring truncation have been explored to enhance its pharmacological properties. In this study, the design and straightforward synthesis of a series of B, C, and E (BCE)-ring-truncated deguelin analogues with deoxybenzoin backbone were described. The structure–activity relationships (SARs) were established by evaluation of their inhibitory activities against three cancer cell lines, A549 (adenocarcinomic human alveolar basal epithelial cells), HCT116 (human colorectal cancer cells), and MCF-7 (breast cancer cells). Six derivatives demonstrated significant and selective inhibitory activities. The ketone derivative **3a** showed potency against A549 ( $IC_{50} = 6.62 \mu M$ ) while the oxime analogue **6a** and D-ring-benzylated ketone analogue **8d** exhibited activity against HCT116 ( $IC_{50} = 3.43$  and  $6.96 \mu M$ , respectively). Moreover, the D-ring alkylated derivatives **8c** and **8e–f** were active against MCF-7 cells ( $IC_{50} < 10 \mu M$ ). The potential suitability of the BCE-ring-truncated deguelin derivatives for drug development was further supported by the favorable *in silico* prediction of their physicochemical properties, druglikeness, and toxicity. This study could provide valuable insights for the further development of novel anticancer agents.



## 1. INTRODUCTION

Deguelin (Figure 1) is a naturally occurring rotenoid<sup>1</sup> that was originally used as pesticide and fish poison.<sup>2</sup> It has emerged as

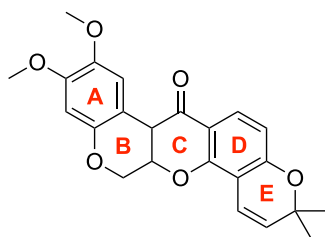


Figure 1. Structure of deguelin with designated A–E-rings.

a promising lead compound for therapeutic optimization and development due to its remarkable antiproliferative activity and unique mechanism of action.<sup>3</sup> Its favorable biological activity has been attributed to its role in regulating various tumor cell signaling transduction pathways. The ability of deguelin to induce apoptosis, inhibit cell proliferation, and promote tumor death is correlated to targeting mitogen-activated protein kinase (MAPK) and phosphatidylinositol 3-kinase (PI3K)/Akt signal transduction cascades.<sup>4</sup> Recent studies show that unlike other heat shock protein 90 (HSP90) inhibitors, deguelin binds to the C-terminal of ATP-binding pocket of HSP90.<sup>5</sup>

This leads to the downregulation of client proteins, including p53 (tumor suppressor protein), CDK4 (associated with cancer prognosis), Akt (critical for cancer cell survival), and hypoxia-inducible factor 1 $\alpha$  (HIF-1 $\alpha$ , involved in oxygen regulation), thus suppressing cell propagation and malignant transformation.<sup>6</sup>

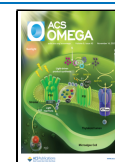
The potential of deguelin as an anticancer agent has been extensively studied;<sup>7</sup> however, its clinical utility has been hindered by concerning *in vivo* toxicity.<sup>8</sup> Derivatization of deguelin to improve its pharmacological profiles and establish structure–activity relationships (SARs) has been previously investigated. Carbonyl group,<sup>9</sup> A- and E-ring modifications,<sup>9b,10</sup> and B- and/or C-ring truncation<sup>9b,11</sup> were the major focus of structural alterations of deguelin. In the study of Chang et al., carbonyl, A-, and E-ring-modified deguelin analogues were reported to be potent HSP90 inhibitors.<sup>9b</sup> However, the complex five-fused rings of deguelin present a great challenge to its total synthesis and limit its accessibility

Received: September 2, 2023

Revised: October 16, 2023

Accepted: October 18, 2023

Published: November 2, 2023



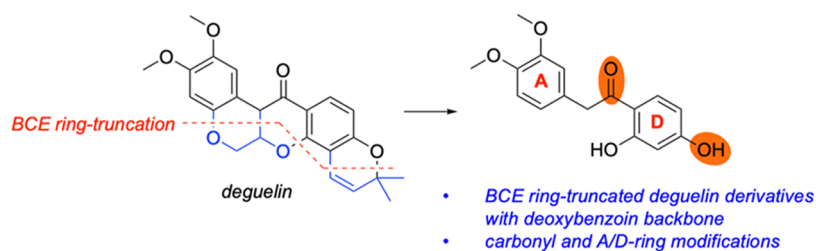
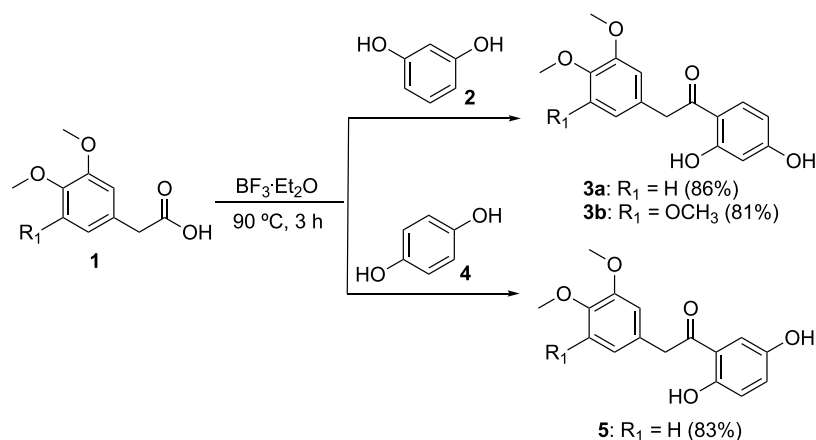
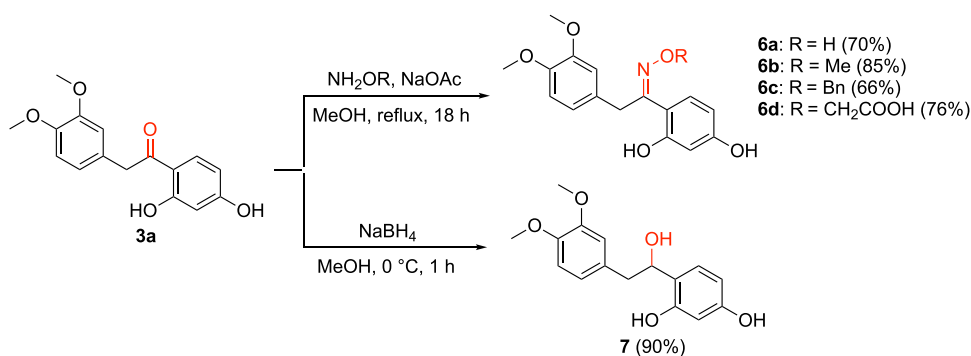


Figure 2. Design strategy for the BCE-ring truncation of deguelin.

### Scheme 1. Synthesis of BCE-Ring-Truncated Ketone Derivatives 3 and 5



### Scheme 2. Synthesis of Carbonyl-Modified BCE-Ring-Truncated Deguelin Derivatives 6 and 7



for further modifications. The presence of B- and C-rings also restrict the conformational flexibility of deguelin, consequently diminishing its potential interaction with HSP90.<sup>11m</sup> To address this challenge, Chang et al. introduced a ring truncation strategy to derive simpler and more synthetically accessible scaffolds. Through this approach, they successfully developed novel analogues of deguelin with truncated B- and/or C-rings which showed antiproliferative properties against H1299 nonsmall-cell lung cancer cell line and antiangiogenic activities in zebrafish embryos.<sup>9b</sup> Kim et al., on the other hand, delved into the SAR studies of C-ring-truncated deguelin derivatives by varying the carbonyl group linker, A/B-, and D/E-rings.<sup>11k</sup> The derivatives exhibited HIF-1 $\alpha$  and antitumor properties against the H1299 cell line. In the SAR studies conducted by Yao et al. on the deguelin derivatives with truncated B- and BC-rings as HSP90 inhibitors, they have established the importance of the methoxy groups at A-ring and the nonessential nature of the alkene moiety at the E-ring.<sup>11h</sup> The choice of functional groups linking the A- and D-rings could yield analogues with varying degrees of potency.

Despite reports on the truncated frameworks of deguelin, the SARs pertaining to the truncation of the BCE-ring in deguelin have not been previously explored. In this study, the design of deguelin analogues was further simplified by truncating B-, C-, and E-rings (Figure 2) resulting in compounds with a deoxybenzoin backbone. Deoxybenzoin derivatives have been known for various biological properties,<sup>12</sup> including antioxidant,<sup>13</sup> antibacterial,<sup>14</sup> immunosuppressive,<sup>15</sup> and anti-inflammatory activities.<sup>15,16</sup> To the best of our knowledge, there are no previous studies of their potential anticancer properties. Thus, the facile synthesis of 15 deoxybenzoin or BCE-ring-truncated analogues was described. Their inhibitory properties against A549 lung cancer cells, HCT116 colorectal cancer cells, and MCF-7 breast cancer cells were evaluated using MTT assay.<sup>17</sup> SAR analysis was conducted by a carbonyl group and A- and D-ring modifications. The physicochemical properties, druglikeness, and toxicity of the derivatives were analyzed using SwissAMDE<sup>18</sup> and ProTox-IL.<sup>19</sup>

## Scheme 3. Synthesis of Monoalkylated BCE-Ring-Truncated Deguelin Derivatives 8 and 9 (X = Cl or Br)

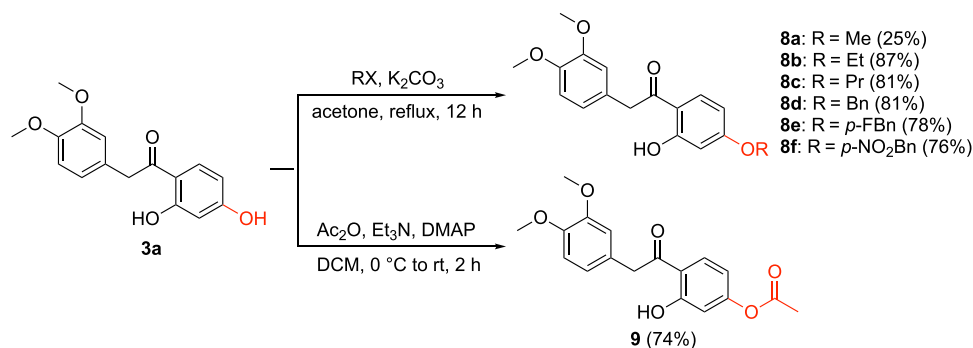


Table 1. ADME-Tox Predictions of BCE-Ring-Truncated Deguelin Derivatives

compound	$M_w$	$n_{RB}$	$n_{HBA}$	$n_{HBD}$	TPSA	$i \log P$	GI absorption	Lipinski's violation	LD <sub>50</sub> (mg/kg)	class
3a	288.3	5	5	2	76.0	1.7	high	0	1520	IV
3b	318.3	6	6	2	85.2	1.9	high	0	1520	IV
5	288.3	5	5	2	76.0	2.0	high	0	2000	IV
6a	303.3	5	6	3	91.5	2.1	high	0	2000	IV
6b	317.3	6	6	2	80.5	2.6	high	0	2000	IV
6c	393.4	8	6	2	80.5	3.3	high	0	2000	IV
6d	361.4	8	8	3	117.8	1.7	high	0	2000	IV
7	290.3	5	5	3	79.1	2.2	high	0	1000	IV
8a	302.3	6	5	1	65.0	2.9	high	0	1520	IV
8b	316.4	7	5	1	65.0	3.4	high	0	1520	IV
8c	330.4	8	5	1	65.0	3.3	high	0	1520	IV
8d	378.4	8	5	1	65.0	3.6	high	0	1520	IV
8e	396.4	8	6	1	65.0	3.5	high	0	1520	IV
8f	423.4	9	7	1	110.8	3.2	high	0	2000	IV
9	330.3	7	6	1	82.1	2.3	high	0	1520	IV

## 2. RESULTS AND DISCUSSION

**2.1. Synthesis of BCE-Ring-Truncated Deguelin Analogues.** As shown in Scheme 1, BCE-ring-truncated deguelin analogues 3 and 5 were initially synthesized following a modified Friedel–Crafts acylation reaction between substituted phenylacetic acid and dihydroxybenzene using boron trifluoride ethyl etherate complex as Lewis acid.<sup>11h</sup> The ketone derivatives 3a–b and 5 were successfully synthesized in very good yields.

Subsequent modifications of the carbonyl group of the ketone derivative 3a were conducted by following the procedures outlined in Scheme 2. Treatment of 3a with the appropriate hydroxyl and alkoxy amines produced oxime and alkylated oxime derivatives 6a–d. Oxime analogue 6a was obtained when 3a was treated with hydroxylamine hydrochloride and NaOAc in MeOH.<sup>20</sup> The synthesis of the alkylated oxime derivatives 6b–d was achieved by treating 3a with methoxy-, *O*-benzyl-, and (carboxymethyl)hydroxyl-amine hydrochloride, respectively. Derivative 3a was reduced to alcohol derivative 7 in 90% yield using NaBH<sub>4</sub> as the reducing agent.

Modifications at the D-ring moiety were also explored by selective alkylation of the *p*-hydroxy group (Scheme 3).<sup>11h</sup> The ketone derivative 3a was treated with various primary alkyl halides to obtain *O*-alkylated derivatives 8a–f via the S<sub>N</sub>2 reaction. *O*-Acylated derivative 9 was produced using acetic anhydride, Et<sub>3</sub>N, and DMAP in DCM. The analogues were obtained in good yields and characterized by using various techniques such as <sup>1</sup>H and <sup>13</sup>C nuclear magnetic resonance

(NMR) spectroscopy and high-resolution mass spectrometry (HRMS).

**2.2. *In Silico* Prediction of ADME-Tox Properties of BCE-Ring-Truncated Deguelin Derivatives.** Table 1 shows the predicted absorption, distribution, metabolism, excretion, and toxicity (ADME-Tox) properties of the synthesized compounds using SwissADME<sup>18</sup> and ProTox-II.<sup>19</sup> The molecular weights ( $M_w < 500$ ), number of rotatable bonds ( $n_{RB} \leq 10$ ), number of hydrogen bond acceptors ( $n_{HBA} \leq 10$ ) and donors ( $n_{HBD} \leq 5$ ), and topological polar surface area ( $20 < TPSA < 130 \text{ \AA}^2$ ) of the compounds were all below the threshold. The lipophilicity values ( $i \log P \leq 5$ ) were around 1.7 to 3.6, indicating the good permeability of the compounds to cell membrane.<sup>21</sup> Moreover, the synthesized analogues showed high gastrointestinal absorption with no violations of Lipinski's rule of five, suggesting its good oral bioavailability. In addition to the ADME properties of the compounds, their acute mammalian toxicity was also predicted using ProTox-II.<sup>19</sup> Indicated by their lethal dose 50 (LD<sub>50</sub>) values ranging from 1000 to 2000 mg/kg, the synthesized BCE-ring-truncated analogues were categorized as Class IV (2000 mg/kg > LD<sub>50</sub> > 300 mg/kg) compounds, implying low adverse effects.

**2.3. Antiproliferative Activities against A549, HCT116, and MCF-7 Cells.** The synthesized derivatives were evaluated for their inhibitory activities *in vitro* using MTT assay.<sup>17</sup> MTT assay is used to measure the cellular metabolic activity of the derivatives as an indicator of their inhibition efficacy against three cancer cell lines (A549 adenocarcinoma human alveolar basal epithelial cells, HCT116 human

colorectal cancer cells, and MCF-7 breast cancer cells). The half-maximal inhibitory concentrations ( $IC_{50}$ ) were measured for all derivatives using deguelin and doxorubicin as the positive controls. Table 2 shows the mean  $IC_{50}$  values of the derivatives ( $n = 3$ ). Compounds that exhibit  $IC_{50} < 10 \mu M$  against one or more of the cell lines used were considered biologically active.<sup>22</sup>

MTT assay revealed that among the derivatives tested, compound **3a** is the only active derivative against A549 cancer cells with an  $IC_{50}$  value of  $6.62 \mu M$  (Table 2). Interestingly, it is slightly more potent than doxorubicin ( $IC_{50} = 7.38 \mu M$ ), a known anticancer drug, and has comparable potency with deguelin ( $IC_{50} = 6.47 \mu M$ ), a known potent compound against lung cancer cells.<sup>23</sup> Derivative **5**, on the other hand, a structural isomer of **3a**, did not exhibit inhibitory activity against the A549 cancer cell line.

Modifications at the carbonyl group, such as conversion to its oxime (**6a**), alkylloxime (**6b–d**), and alcohol (**7**) derivatives, generally led to decreased potency against the A549 cell line. Introducing alkyl substituents in the *p*-hydroxy group of the D-ring also decreased the inhibitory activities of compound **3a**. Notably, a 2-fold decrease in the potency of compound **3a** was observed when *O*-methylated (**8a**,  $IC_{50} = 15.2 \mu M$ ). Further decrease in inhibitory property was observed when the substituents become bulkier, *i.e.*, ethyl (**8b**,  $35.1 \mu M$ ) and propyl (**8c**,  $88.7 \mu M$ ) groups. No potent activity was observed for compounds containing benzyl derivatives (**8d–e**).

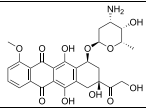
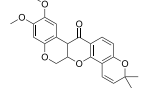
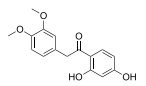
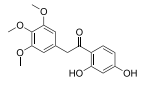
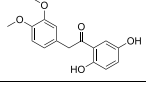
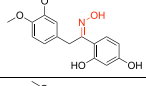
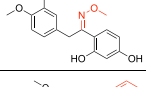
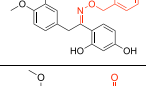
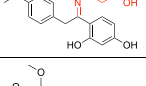
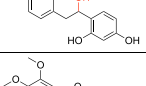
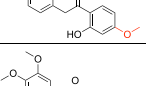
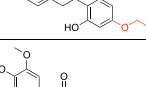
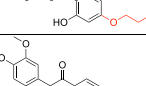
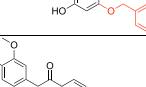
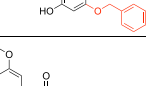
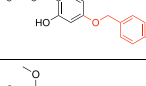
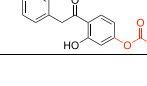
The inhibitory properties of the derivatives were assessed against HCT116 human colorectal cancer cells. As presented in Table 2, the oxime derivative **6a** displayed higher potency ( $IC_{50} = 3.43 \mu M$ ) than deguelin ( $IC_{50} = 26.2 \mu M$ ) and doxorubicin ( $IC_{50} = 6.41 \mu M$ ). However, substitution of the hydroxy moiety of **6a** resulted in a loss of activity [ $IC_{50} = 93.3 \mu M$  for methylloxime (**6b**) and  $30.2 \mu M$  for benzyloxime (**6c**) derivative]. These results suggest that the hydroxy moiety of the oxime derivative plays a crucial role in its antiproliferative property against colon cancer cells. Moreover, compound **7**, the alcohol analogue of compound **3a**, did not exhibit an inhibitory activity.

In contrast to the trend observed in oxime derivatives, alkylation of the *p*-hydroxy group of the D-ring of **3a** led to a significant increase in potency. Bulky groups proved to be beneficial in enhancing the potency of *O*-alkylated derivatives against HCT116 cancer cells. Compound **8a** (*O*-methylated) for instance, gave an  $IC_{50}$  value of  $68.7 \mu M$ , while compounds with propyl (**8c**) and benzyl (**8d**) groups exhibited even greater potency with  $IC_{50}$  values of 13.3 and  $6.96 \mu M$ , respectively. Acylated compound **9**, however, was inactive, as it showed an  $IC_{50}$  value  $>100 \mu M$ .

The derivatives were also evaluated against MCF-7 breast cancer cell lines (Table 2). The parent compound **3a** is inactive against MCF-7 cells ( $IC_{50} > 10 \mu M$ ), whereas the other ketone derivatives **3b** and **5** displayed better  $IC_{50}$  values of 36.0 and  $40.2 \mu M$ , respectively. These findings indicate that the position of the OH group and the presence of an additional  $-OCH_3$  group could be important factors in improving the antiproliferative activity against breast cancer cells. Similarly, all of the oxime derivatives **6a–c** and alcohol analogue **7** lacked efficacy against breast cancer cells.

Similar to the trend observed in the HCT116 cell line, there was a dramatic increase in the antiproliferative activity against MCF-7 cancer cells upon the *O*-alkylation of compound **3a**. Increasing the carbon chain length resulted in improved

**Table 2.** Experimentally Measured  $IC_{50}$  Values of BCE-Ring-Truncated Deguelin Derivatives against A549, HCT116, and MCF-7 Cancer Cell Lines

Compounds <sup>a</sup>	Structure	$IC_{50}$ ( $\mu M$ ) <sup>b</sup>		
		A549	HCT 116	MCF-7
Doxorubicin		7.38	6.41	5.89
Deguelin		6.47	26.2	33.8
<b>3a</b>		6.62	>100	>100
<b>3b</b>		70.9	30.0	36.0
<b>5</b>		>100	n.s. <sup>b</sup>	40.2
<b>6a</b>		>100	3.43	65.6
<b>6b</b>		>100	93.3	94.1
<b>6c</b>		20.8	30.2	32.0
<b>6d</b>		>100	n.s. <sup>b</sup>	n.s. <sup>b</sup>
<b>7</b>		>100	>100	95.5
<b>8a</b>		15.2	68.7	43.4
<b>8b</b>		35.1	n.s. <sup>b</sup>	11.0
<b>8c</b>		88.7	13.3	5.09
<b>8d</b>		>100	6.96	12.0
<b>8e</b>		44.8	n.s. <sup>b</sup>	4.36
<b>8f</b>		12.3	n.s. <sup>b</sup>	8.41
<b>9</b>		n.s. <sup>b</sup>	>100	82.5

<sup>a</sup>All compounds were purified using column chromatography. <sup>b</sup> $IC_{50}$  values were determined as the mean of triplicate experiments. <sup>c</sup>n.s. =

Table 2. continued

nonsigmoidal means that the compound does not follow the sigmoidal fit curve; thus, IC<sub>50</sub> cannot be determined.

activity, with *O*-propylated compound **8c** (IC<sub>50</sub> = 5.09 μM) showing the highest potency. Remarkably, it exhibited higher activity than deguelin (IC<sub>50</sub> = 33.8 μM) and doxorubicin (IC<sub>50</sub> = 5.89 μM). Introducing a much bulkier benzyl group (**8d**, IC<sub>50</sub> = 12.0 μM) decreased the activity by 2-fold. However, the presence of deactivating substituents in the *para* position of the benzyl group improves their potency [*p*-fluorobenzyl- (**8e**), IC<sub>50</sub> = 4.36 μM and *p*-nitrobenzyl- (**8f**), IC<sub>50</sub> = 8.41 μM]. *O*-Acetylated derivative **9** did not show antiproliferative activity against breast cancer cells.

In summary, a total of six BCE-ring-truncated deguelin derivatives—**3a**, **6a**, **8c**, **8d**, **8e**, and **8f**—were identified to have potent (IC<sub>50</sub> < 10 μM) inhibitory activities against the cancer cell lines tested. Addition of alkyl groups to the *p*-hydroxy of the D-ring of **3a** generally enhanced the inhibitory activity. Alkylation of the oxime derivative **6a** on the other hand was not advantageous, as the alkyloxime analogues did not show potency against all three cancer cell lines.

### 3. CONCLUSIONS

The facile synthesis of a series of structurally simple BCE-ring-truncated deguelin derivatives (**3a–9**) bearing a deoxybenzoin backbone is presented in this study. Their antiproliferative activities against three cancer cell lines (A549, HCT116, and MCF-7) were investigated using MTT assay. The structure–activity relationship was explored by generating carbonyl-containing derivatives with substituted A- and D-rings, modifying the carbonyl group to oxime, alkyloxime, and alcohol derivatives and *O*-alkylation of the D-ring. Six out of the 15 compounds studied, namely, **3a**, **6a**, **8c**, **8d**, **8e**, and **8f**, displayed enhanced and selective antiproliferative activities. The ketone derivative **3a** demonstrated potency against A549 (IC<sub>50</sub> = 6.62 μM), whereas oxime analogue **6a** and D-ring-benzylated ketone analogue **8d** exhibited activity against HCT116 (IC<sub>50</sub> = 3.43 and 6.96 μM, respectively). Furthermore, the D-ring-alkylated derivatives **8c** and **8e–f** were active against MCF-7 cells (IC<sub>50</sub> < 10 μM). *In silico* analysis of the physicochemical properties and toxicity of the derivatives revealed druglike attributes that are within predefined thresholds. The promising *in vitro* assay results and favorable predicted ADME-Tox properties indicate the potential of these derivatives as anticancer agents. Ongoing and future work includes *in vivo* and ADME-Tox assays to validate their efficacy and safety and conducting comprehensive biological assays and in-depth mechanistic studies.

### 4. EXPERIMENTAL SECTION

**4.1. General Information.** All reagents were purchased and used as received, unless otherwise specified. <sup>1</sup>H and <sup>13</sup>C NMR spectra were recorded on a Varian 500 MHz spectrometer using deuterated dimethyl sulfoxide (DMSO-*d*<sub>6</sub>). <sup>1</sup>H and <sup>13</sup>C chemical shifts are expressed in parts per million (ppm) and are referenced at 2.50 and 39.5 ppm, respectively. Data are presented as follows: chemical shift (δ), multiplicity (s = singlet, d = doublet, dd = doublet of doublet, t = triplet, q = quartet, and m = multiplet), coupling constants (J) in Hz, and integration. The exact mass was analyzed using a

Waters Acquity UPLC H-Class-Xevo G2XS Quadrupole Time-of-Flight High-Resolution Mass Spectrometer in positive ion mode electrospray ionization. Melting points were determined using a Cole Parmer Electrochemical IA9200 and reported as uncorrected.

#### 4.2. Synthesis of BCE-Ring-Truncated Deguelin Derivatives. 4.2.1. General Method for the Preparation of Compounds **3a–b** and **5**.

Compounds **3a–b** and **5** were prepared following the Friedel–Crafts acylation procedure reported by Yao et al.<sup>11h</sup> Phenylacetic acid (1.0 g, 1.0 equiv), dihydroxybenzene (1.0 equiv), and boron trifluoride ethyl etherate (15 mL) were placed in a round-bottom flask and stirred at 90 °C for 3 h under N<sub>2</sub> gas. Afterward, an ample amount of ice-cold 10% aqueous sodium acetate solution was added to the reaction mixture to precipitate out the product. The precipitate was collected by vacuum filtration and purified by column chromatography in a gradient elution of ethyl acetate/*n*-hexane (0:100 → 30:70) to obtain the ketone derivatives.

**4.2.1.1. 1-(2,4-Dihydroxyphenyl)-2-(3,4-dimethoxyphenyl)ethanone (**3a**).** Using 2-(3,4-dimethoxyphenyl)acetic acid (1.0 g, 5.1 mmol, 1.0 equiv) and resorcinol (0.56 g, 5.1 mmol, 1.0 equiv), compound **3a** was obtained as a pale yellow solid (1.3 g, 86% yield). The isolated compound matched the reported <sup>1</sup>H NMR data.<sup>11h</sup> MP = 178 °C; <sup>1</sup>H NMR (500 MHz, DMSO-*d*<sub>6</sub>) δ 12.9 (s, 1H), 10.73 (s, 1H), 7.95 (d, J = 8.6 Hz, 1H), 6.90 (s, 1H), 6.87 (d, J = 7.9 Hz, 1H), 6.78 (d, J = 7.9 Hz, 1H), 6.38 (d, J = 8.6 Hz, 1H), 6.25 (s, 1H), 4.19 (s, 2H), 3.71 (s, 6H). <sup>13</sup>C NMR (126 MHz, DMSO-*d*<sub>6</sub>) δ: 202.5, 165.2, 164.8, 148.7, 147.7, 133.7, 127.6, 121.6, 113.4, 112.2, 111.9, 108.4, 102.6, 55.6, 55.6, 43.8. HRMS (ESI) *m/z*: calcd for [M + H]<sup>+</sup> C<sub>16</sub>H<sub>17</sub>O<sub>5</sub>: 289.1071, found: 289.1076.

**4.2.1.2. 1-(2,4-Dihydroxyphenyl)-2-(3,4,5-trimethoxyphenyl)ethanone (**3b**).** Using 2-(3,4,5-trimethoxyphenyl)acetic acid (63.3 mg, 0.28 mmol, 1.0 equiv) and resorcinol (17.7 mg, 0.28 mmol, 1.0 equiv), **3b** was obtained as a white solid (89.1 mg, 81% yield). MP = 180 °C; <sup>1</sup>H NMR (500 MHz, DMSO-*d*<sub>6</sub>) δ 12.5 (s, 1H), 10.7 (s, 1H), 7.96 (d, J = 8.9 Hz, 1H), 6.61 (s, 2H), 6.40 (dd, J = 2.3, 8.9 Hz, 1H), 6.26 (d, J = 2.3 Hz, 1H), 4.21 (s, 2H), 3.73 (s, 6H), 3.63 (s, 3H). <sup>13</sup>C NMR (126 MHz, DMSO-*d*<sub>6</sub>) δ 202.0, 165.0, 164.6, 152.8, 136.2, 133.5, 130.7, 112.2, 108.3, 107.0, 102.5, 60.0, 55.9, 44.3, 39.5. HRMS (ESI) *m/z*: calcd for [M + H]<sup>+</sup> C<sub>17</sub>H<sub>19</sub>O<sub>6</sub>: 319.1181, found: 319.1209.

**4.2.1.3. 1-(2,5-Dihydroxyphenyl)-2-(3,4-dimethoxyphenyl)ethanone (**5**).** Using 2-(3,4-dimethoxyphenyl)acetic acid (50.0 mg, 0.28 mmol, 1.0 equiv) and hydroquinone (17.7 mg, 0.28 mmol, 1.0 equiv), **5** was obtained as a pale yellow solid (83.8 mg, 83% yield). MP = 125 °C; <sup>1</sup>H NMR (500 MHz, DMSO-*d*<sub>6</sub>) δ = 9.47 (s, 1H), 8.65 (s, 1H), 6.96 (d, J = 1.9 Hz, 1H), 6.92 (d, J = 8.3 Hz, 1H), 6.89 (dd, J = 8.9, 2.3 Hz, 1H), 6.87 (dd, J = 8.2, 1.9 Hz, 1H), 6.76 (dd, J = 8.9, 2.3 Hz, 1H), 6.57 (s, 1H), 3.81 (s, 2H), 3.75 (s, 3H), 3.74 (s, 3H). <sup>13</sup>C NMR (126 MHz, DMSO-*d*<sub>6</sub>) δ: 170.7, 155.0, 149.8, 148.6, 147.9, 142.7, 126.4, 122.4, 121.5, 115.7, 115.6, 113.2, 111.8, 55.5, 55.5, 39.7. HRMS (ESI) *m/z*: calcd [M + H]<sup>+</sup> C<sub>16</sub>H<sub>17</sub>O<sub>5</sub>: 304.1180, found: 304.1212.

**4.2.2. General Procedure for the Preparation of Compounds **6a–d**.** Following the procedure reported by Zhao et al.,<sup>20</sup> hydroxylamine/alkoxyamine hydrochloride (1.2 equiv) and sodium acetate (1.2 equiv) were added to a 10 mL round-bottom flask containing a solution of **3a** (1.0 equiv) in

dry methanol (5 mL). The mixture was stirred for 18 h at 65 °C and then cooled to room temperature. The resulting solution was treated with water and extracted with ethyl acetate (3 × 10 mL). The combined organic phases were dried over magnesium sulfate, and the solvent was removed *in vacuo*. The collected solid was purified by column chromatography in a gradient elution of ethyl acetate/*n*-hexane (0:100 → 35:65) to obtain the oxime/alkyloxime analogues.

**4.2.2.1. 1-(2,4-Dihydroxyphenyl)-2-(3,4-dimethoxyphenyl)ethanone Oxime (6a).** Hydroxylamine hydrochloride (24.3 mg) was used to obtain **6a** as a white solid (74.3 mg, 70% yield). MP = 202 °C; <sup>1</sup>H NMR (500 MHz, DMSO-*d*<sub>6</sub>) δ 11.79 (s, 1H), 11.45 (s, 1H), 9.72 (s, 1H), 7.32 (d, *J* = 8.6 Hz, 1H), 6.92 (d, *J* = 1.9 Hz, 1H), 6.82 (d, *J* = 8.3 Hz, 1H), 6.73 (dd, *J* = 8.2, 1.9 Hz, 1H), 6.27 (d, *J* = 2.5 Hz, 1H), 6.25 (s, 1H), 4.10 (s, 2H), 3.70 (s, 3H), 3.68 (s, 3H). <sup>13</sup>C NMR (126 MHz, DMSO-*d*<sub>6</sub>) δ: 159.4, 159.4, 159.3, 148.7, 147.3, 129.5, 129.3, 120.2, 112.6, 112.0, 110.0, 105.9, 103.0, 55.5, 55.4, 29.4. HRMS (ESI) *m/z*: calcd for [M + H]<sup>+</sup> C<sub>16</sub>H<sub>18</sub>NO<sub>5</sub>: 304.1180, found: 304.1212.

**4.2.2.2. 1-(2,4-Dihydroxyphenyl)-2-(3,4-dimethoxyphenyl)ethanone O-Methyloxime (6b).** Methoxyamine hydrochloride (35.1 mg) was used to obtain **6b** as a pale yellow solid (94.4 mg, 85% yield). MP = 151 °C; <sup>1</sup>H NMR (500 MHz, DMSO-*d*<sub>6</sub>) δ 11.04 (s, 1H), 9.85 (s, 1H), 7.29 (d, *J* = 8.4, 1H), 6.86 (s, 1H), 6.82 (d, *J* = 8.1 Hz, 1H), 6.66 (d, *J* = 3.2 Hz, 1H), 6.26 (d, *J* = 7.1 Hz, 2H), 4.07 (s, 2H), 3.95 (s, 3H), 3.69 (s, 3H), 3.67 (s, 3H). <sup>13</sup>C NMR (126 MHz, DMSO-*d*<sub>6</sub>) δ: 160.1, 159.9, 159.0, 148.7, 147.3, 130.2, 128.7, 112.3, 111.9, 109.7, 107.2, 103.0, 62.0, 55.5, 55.4, 30.5. HRMS (ESI) *m/z*: calcd for [M + H]<sup>+</sup> C<sub>17</sub>H<sub>20</sub>NO<sub>5</sub>: 318.1336, found: 318.1340.

**4.2.2.3. 1-(2,4-Dihydroxyphenyl)-2-(3,4-dimethoxyphenyl)ethanone O-Benzoyloxime (6c).** *O*-Benzylhydroxylamine hydrochloride (165.2 mg) was used to obtain **6c** as a pale yellow solid (90.9 mg, 66% yield). MP = 140 °C; <sup>1</sup>H NMR (500 MHz, DMSO-*d*<sub>6</sub>) δ 10.96 (s, 1H), 7.42–7.30 (m, 6H), 6.83 (s, 1H), 6.80 (d, *J* = 8.3 Hz, 1H), 6.68 (d, *J* = 8.3 Hz, 1H), 6.28 (m, 2H), 5.20 (s, 2H), 4.11 (s, 2H), 3.67 (s, 3H), 3.61 (s, 3H). <sup>13</sup>C NMR (126 MHz, DMSO-*d*<sub>6</sub>) δ: 160.4, 160.0, 159.1, 148.8, 147.4, 137.4, 130.2, 128.8, 128.6, 128.5, 128.2, 120.4, 112.4, 112.0, 109.7, 107.4, 103.1, 75.8, 55.5, 55.4, 30.6. HRMS (ESI) *m/z*: calcd for [M + H]<sup>+</sup> C<sub>23</sub>H<sub>24</sub>NO<sub>5</sub>: 395.1732, found: 395.1702.

**4.2.2.4. 2-(((1-(2,4-Dihydroxyphenyl)-2-(3,4-dimethoxyphenyl)ethylidene)amino)oxy)acetic Acid (6d).** *O*-(Carboxymethyl)hydroxylamine hemihydrochloride (151.8 mg) was used to obtain **6d** as a pale yellow solid (96.1 mg, 76% yield). MP = 189 °C; <sup>1</sup>H NMR (500 MHz, DMSO-*d*<sub>6</sub>) δ 10.7 (s, 1H), 9.93 (s, 1H), 7.27 (d, *J* = 7.5, 1H), 6.98 (s, 1H), 6.79 (s, 2H), 6.26 (m, 2H), 4.73 (s, 2H), 4.11 (s, 2H), 3.68 (s, 3H), 3.66 (s, 3H). <sup>13</sup>C NMR (126 MHz, DMSO-*d*<sub>6</sub>) δ: 171.4, 160.7, 160.1, 159.0, 149.0, 147.6, 130.6, 129.0, 120.8, 112.6, 112.1, 110.0, 107.6, 103.3, 70.8, 55.7, 31.0. HRMS (ESI) *m/z*: calcd for [M + H]<sup>+</sup> C<sub>18</sub>H<sub>20</sub>NO<sub>5</sub>: 362.1240, found: 362.1239.

**4.2.3. Procedure for the Synthesis of 4-(2-(3,4-Dimethoxyphenyl)-1-hydroxyethyl)benzene-1,3-diol (7).** Sodium borohydride (53 mg, 1.4 mmol, 4.0 equiv) was added to a solution of **3a** (100 mg, 0.35 mmol, 1.0 equiv) in dry methanol (5 mL) at 0 °C. The reaction was monitored using TLC. After completion, the reaction was quenched with saturated ammonium chloride solution, treated with water, and extracted with ethyl acetate (3 × 10 mL). The combined organic phase

was dried over magnesium sulfate, and the solvent was removed *in vacuo* to afford **7** as a white solid powder (100 mg, 90% yield). No further purification was performed. MP = 262 °C (decomposed); <sup>1</sup>H NMR (500 MHz, DMSO-*d*<sub>6</sub>) δ 9.24 (s, 1H), 9.13 (s, 1H), 7.00 (d, *J* = 7.9 Hz, 1H), 6.78 (d, *J* = 7.1 Hz, 1H), 6.67 (s, 1H), 6.66 (m, 2H), 6.20 (s, 1H), 6.17 (d, *J* = 8.1, 1H), 4.94 (t, *J* = 4.9 Hz, 1H), 4.89 (s, 1H), 3.68 (s, 3H), 3.65 (s, 3H), 2.79 (dd, *J* = 13.7, 8.1, 1H), 2.64 (dd, *J* = 7.9, 3.0 Hz, 1H). <sup>13</sup>C NMR (126 MHz, DMSO-*d*<sub>6</sub>) δ: 157.1, 155.1, 148.4, 147.3, 132.7, 127.8, 122.8, 121.8, 113.7, 111.9, 106.4, 102.6, 69.1, 55.9, 55.7, 44.1. HRMS (ESI) *m/z*: calcd for [M – OH]<sup>+</sup> C<sub>16</sub>H<sub>17</sub>NO<sub>4</sub>: 273.1132, found: 273.1125.

**4.2.4. General Procedure for the Preparation of Compounds 8a–f.** *O*-Alkylated derivatives **8a–f** were prepared following the methylation procedure reported by Yao et al.<sup>11h</sup> The alkyl halide (1.0 equiv) and potassium carbonate (1 equiv) were added to a 10 mL round-bottom flask containing a solution of **3a** (100 mg, 0.35 mmol, 1.0 equiv) in dry acetone (5 mL), and the mixture was heated under reflux for 12 h. The mixture was then allowed to cool to room temperature. The solvent was removed under reduced pressure, and the residue was treated with water and extracted with ethyl acetate (3 × 10 mL). The combined organic phase was dried over magnesium sulfate, and the solvent was removed *in vacuo*. The crude residue was purified by column chromatography in a gradient elution of ethyl acetate/*n*-hexane (0:100 → 25:75) to obtain the mono-*O*-alkyl derivatives.

**4.2.4.1. 2-(3,4-Dimethoxyphenyl)-1-(4-methoxy-2-hydroxyphenyl)ethanone (8a).** Methyl iodide (21.8 μL) was used to obtain **8a** as a white solid (26.4 mg, 25% yield). MP = 121 °C; <sup>1</sup>H NMR (500 MHz, DMSO-*d*<sub>6</sub>) δ 12.59 (s, 1H), 8.02 (d, *J* = 9.0 Hz, 1H), 6.90 (d, *J* = 1.9 Hz, 1H), 6.87 (d, *J* = 8.3 Hz, 1H), 6.78 (dd, *J* = 1.8, 8.2 Hz, 1H), 6.53 (dd, *J* = 2.5, 9.0 Hz, 2H), 6.47 (d, *J* = 2.5 Hz, 1H), 4.24 (s, 2H), 3.81 (s, 3H), 3.71 (s, 3H), 3.71 (s, 3H). <sup>13</sup>C NMR (126 MHz, DMSO-*d*<sub>6</sub>) δ 202.8, 165.7, 164.5, 148.6, 147.7, 133.1, 127.3, 121.6, 113.4, 113.1, 111.9, 109.6, 107.4, 100.9, 55.8, 55.1, 55.48, 43.9. HRMS (ESI) *m/z*: calcd for [M + H]<sup>+</sup> C<sub>18</sub>H<sub>19</sub>O<sub>5</sub>: 303.1232, found: 303.1257.

**4.2.4.2. 2-(3,4-Dimethoxyphenyl)-1-(4-ethoxy-2-hydroxyphenyl)ethanone (8b).** Ethyl iodide (28.1 μL) was used to obtain **8b** as a white solid (96.3 mg, 87% yield). MP = 96 °C; <sup>1</sup>H NMR (500 MHz, DMSO-*d*<sub>6</sub>) δ 12.60 (s, 1H), 8.01 (d, *J* = 9.0 Hz, 1H), 6.91 (d, *J* = 1.9 Hz, 1H), 6.87 (d, *J* = 8.3 Hz, 1H), 6.79 (dd, *J* = 1.8, 6.4 Hz, 1H), 6.52 (dd, *J* = 2.5, 6.5 Hz, 1H), 6.45 (d, *J* = 2.0 Hz, 1H), 4.24 (s, 2H), 4.08 (q, *J* = 7.0 Hz, 2H), 3.72 (s, 3H), 3.71 (s, 3H), 1.32 (t, *J* = 7.0 Hz, 3H). <sup>13</sup>C NMR (126 MHz, DMSO-*d*<sub>6</sub>) δ: 202.7, 165.0, 164.5, 148.6, 147.6, 133.1, 127.3, 121.5, 113.4, 112.9, 111.8, 107.6, 101.3, 63.8, 55.5, 55.4, 43.9, 14.4. HRMS (ESI) *m/z*: calcd for [M + H]<sup>+</sup> C<sub>18</sub>H<sub>21</sub>O<sub>5</sub>: 317.1384, found: 317.1338.

**4.2.4.3. 2-(3,4-Dimethoxyphenyl)-1-(2-hydroxy-4-propoxyphenyl)ethanone (8c).** Propyl iodide (34.0 μL) was used to obtain **8c** as a white solid (93.7 mg, 81% yield). MP = 111 °C; <sup>1</sup>H NMR (500 MHz, DMSO-*d*<sub>6</sub>) δ 12.54 (s, 1H), 8.00 (d, *J* = 9.1 Hz, 1H), 6.92 (d, *J* = 1.9 Hz, 1H), 6.87 (d, *J* = 8.3 Hz, 1H), 6.80 (dd, *J* = 1.8, 6.4 Hz, 1H), 6.52 (dd, *J* = 2.5, 6.5 Hz, 1H), 6.45 (d, *J* = 2.5 Hz, 1H), 4.23 (s, 2H), 3.96 (t, *J* = 6.6 Hz, 2H), 3.73 (s, 3H), 3.71 (s, 3H), 1.70 (m, 2H), 0.95 (t, *J* = 7.5 Hz, 3H). <sup>13</sup>C NMR (126 MHz, DMSO-*d*<sub>6</sub>) δ 202.7, 165.2, 164.6, 148.7, 147.7, 133.1, 129.1, 127.3, 121.5, 113.4, 111.8, 107.6, 101.3, 69.5, 55.4, 43.9, 21.8, 10.2. HRMS (ESI) *m/z*: calcd for [M + H]<sup>+</sup> C<sub>19</sub>H<sub>23</sub>NO<sub>5</sub>: 331.1540, found: 331.1545.

4.2.4.4. 1-(4-(Benzyloxy)-2-hydroxyphenyl)-2-(3,4-dimethoxyphenyl)ethanone (**8d**). Benzyl bromide (41.6  $\mu\text{L}$ ) was used to obtain **8d** as a white solid (107.3 mg, 81% yield). MP = 106  $^{\circ}\text{C}$ ;  $^1\text{H}$  NMR (500 MHz,  $\text{DMSO-}d_6$ )  $\delta$  12.60 (s, 1H), 8.03 (d,  $J = 9.0$  Hz, 1H), 7.44 (d,  $J = 7.7$  Hz, 2H), 7.40 (t,  $J = 7.3$  Hz, 2H), 7.34 (t,  $J = 7.3$  Hz, 1H), 6.92 (s, 1H), 6.87 (d,  $J = 8.2$  Hz, 1H), 6.80 (d,  $J = 8.2$  Hz, 1H), 6.61 (d,  $J = 9.0$  Hz, 1H), 6.57 (s, 1H), 5.18 (s, 2H), 4.24 (s, 2H), 3.72 (s, 3H), 3.71 (s, 3H).  $^{13}\text{C}$  NMR (126 MHz,  $\text{DMSO-}d_6$ )  $\delta$  202.8, 164.7, 164.4, 148.6, 147.7, 136.3, 133.2, 128.5, 128.1, 127.8, 127.3, 121.6, 113.4, 113.2, 111.9, 107.9, 101.9, 69.7, 55.5, 55.5, 43.9. HRMS (ESI)  $m/z$ : calcd for  $[\text{M} + \text{H}]^+$   $\text{C}_{23}\text{H}_{23}\text{NO}_5$ : 379.1540, found: 379.1552.

4.2.4.5. 2-(3,4-Bimethoxyphenyl)-1-(4-(4-fluorobenzyl)-oxy)-2-hydroxyphenyl)ethanone (**8e**). 4-Fluorobenzyl bromide (40.7  $\mu\text{L}$ ) was used to obtain **8e** as a pale yellow solid (108.2 mg, 78% yield). MP = 88  $^{\circ}\text{C}$ ;  $^1\text{H}$  NMR (500 MHz,  $\text{DMSO-}d_6$ )  $\delta$  12.51 (br. s, 1H), 7.97 (d,  $J = 9.1$  Hz, 1H), 7.45 (dt,  $J = 3.1, 6.4$  Hz, 2H), 7.18 (dt,  $J = 2.5, 9.1$  Hz, 2H), 6.84 (m, 2H), 6.75 (dd,  $J = 2.1, 8.2$  Hz, 1H), 6.57 (dd,  $J = 2.5, 9.1$  Hz, 1H), 6.49 (d,  $J = 2.6$  Hz, 1H), 5.11 (s, 2H), 4.18 (s, 2H), 3.67 (s, 6H).  $^{13}\text{C}$  NMR (126 MHz,  $\text{DMSO-}d_6$ )  $\delta$  203.5, 165.1, 164.8, 149.0, 148.1, 133.7, 132.9, 130.7, 130.6, 127.2, 122.1, 116.0, 115.8, 113.7, 113.7, 112.3, 108.5, 102.4, 69.5, 56.0, 56.0, 44.4. HRMS (ESI)  $m/z$ : calcd for  $[\text{M} + \text{H}]^+$   $\text{C}_{23}\text{H}_{22}\text{FO}_5$ : 397.1451, found: 397.1497.

4.2.4.6. 2-(3,4-Dimethoxyphenyl)-1-(2-hydroxy-4-(4-nitrobenzyl)oxy)phenyl)ethanone (**8f**). 4-Nitrobenzyl bromide (41.6  $\mu\text{L}$ ) was used to obtain **8f** as a pale yellow solid (112.6 mg, 76% yield). MP = 148  $^{\circ}\text{C}$ ;  $^1\text{H}$  NMR (500 MHz,  $\text{DMSO-}d_6$ )  $\delta$  12.6 (s, 1H), 8.26 (d,  $J = 8.6$  Hz, 1H), 8.05 (d,  $J = 9.0$  Hz, 2H), 7.71 (d,  $J = 8.6$  Hz, 2H), 6.91 (d,  $J = 1.6$  Hz, 1H), 6.87 (d,  $J = 8.2$  Hz, 1H), 6.79 (dd,  $J = 1.6, 8.2$  Hz, 1H), 6.64 (dd,  $J = 2.4, 9.0$  Hz, 1H), 6.58 (d,  $J = 2.4$  Hz, 1H), 5.37 (s, 2H), 4.25 (s, 2H), 3.71 (s, 3H), 3.71 (s, 3H).  $^{13}\text{C}$  NMR (126 MHz,  $\text{DMSO-}d_6$ )  $\delta$  202.9, 164.3, 164.2, 144.2, 133.3, 128.3, 127.7, 123.7, 121.5, 113.5, 113.4, 111.8, 111.8, 109.6, 107.8, 102.0, 68.4, 55.5, 44.0. HRMS (ESI)  $m/z$ : calcd for  $[\text{M} + \text{H}]^+$   $\text{C}_{23}\text{H}_{22}\text{NO}_7$ : 424.1396, found: 424.1374.

4.2.5. Procedure for the Synthesis of 4-(2-(3,4-Dimethoxyphenyl)acetyl)-3-hydroxyphenyl Acetate (**9**). Following the acylation procedure reported by Yao et al.,<sup>11h</sup> acetic anhydride (41.6  $\mu\text{L}$ , 0.35 mmol, 1.0 equiv) and triethylamine (41.6  $\mu\text{L}$ , 0.35 mmol, 1.0 equiv) were added to a solution of **3a** (100 mg, 0.35 mmol, 1.0 equiv) in dry DCM (5 mL) at 0  $^{\circ}\text{C}$ . A catalytic amount of DMAP was added and stirred for 15 min and then at room temperature for 2 h. After the reaction was completed, saturated sodium bicarbonate solution was added to quench the reaction, treated with water, and extracted with ethyl acetate (3  $\times$  10 mL). The combined organic phase was dried over magnesium sulfate, and the solvent was removed *in vacuo*. The crude residue was purified by column chromatography with a gradient elution of ethyl acetate/*n*-hexane (0:100  $\rightarrow$  25:65) to obtain **9** as a white solid (85.6 mg, 74% yield). MP = 106  $^{\circ}\text{C}$ ;  $^1\text{H}$  NMR (500 MHz,  $\text{DMSO-}d_6$ )  $\delta$  12.1 (s, 1H), 8.08 (d,  $J = 8.6$  Hz, 1H), 6.91 (d,  $J = 1.8$  Hz, 1H), 6.88 (d,  $J = 8.3$  Hz, 1H), 6.79 (dd,  $J = 2.0, 8.2$  Hz, 1H), 6.77 (d,  $J = 2.1$  Hz, 1H), 6.75 (dd,  $J = 2.3, 8.6$  Hz, 1H), 4.33 (s, 2H), 3.72 (s, 6H), 2.27 (s, 3H).  $^{13}\text{C}$  NMR (126 MHz,  $\text{DMSO-}d_6$ )  $\delta$ : 203.0, 168.5, 162.2, 156.0, 148.6, 147.7, 132.6, 126.9, 121.7, 118.1, 113.5, 113.3, 111.8, 110.7, 55.5, 55.4, 45.0, 20.9. HRMS (ESI)  $m/z$ : calcd for  $[\text{M} + \text{H}]^+$   $\text{C}_{18}\text{H}_{19}\text{O}_6$ : 332.1249, found: 332.1220.

4.3. MTT Assay. MTT assay, a colorimetric assay used to analyze the metabolic activity of a cell after exposure to a compound, was used to determine the inhibitory activity of the synthesized compounds against A549 lung cancer, HCT116 human colorectal carcinoma cells, and MCF-7 breast cancer cells. In this assay, doxorubicin served as the positive control, while dimethyl sulfoxide (DMSO) served as the negative control. Adapting the procedure of Mosmann,<sup>17</sup> the cells were seeded in a 96-well plate with a seeding density of 4 or 6  $\times 10^3$  cells/mL and were incubated at 37  $^{\circ}\text{C}$  for 24 h and 5%  $\text{CO}_2$ . The samples were then prepared via 8-fold dilution starting from 100  $\mu\text{g}/\text{mL}$  down to 0.78  $\mu\text{g}/\text{mL}$ . After incubation, each well was treated with the diluted samples and was again incubated for 72 h in a humidified atmosphere in 5%  $\text{CO}_2$  at 37  $^{\circ}\text{C}$ . The spent media was then removed and 10  $\mu\text{L}$  of 5 mg/mL MTT dye in phosphate-buffered solution was added to each well. The plate was incubated again in 5%  $\text{CO}_2$  at 37  $^{\circ}\text{C}$  for 4 h, and 10  $\mu\text{L}$  of DMSO was added to the culture well to solubilize the formazan product. After gentle shaking, the absorbance of each well was measured at 570 nm. The half-maximal inhibitory concentration or  $\text{IC}_{50}$  values were computed by employing a nonlinear regression curve fit on the computed percent inhibition per log concentration of the sample. Compounds with an  $\text{IC}_{50}$  of less than or equal to 10  $\mu\text{M}$  were considered active.

## ■ ASSOCIATED CONTENT

### Supporting Information

The Supporting Information is available free of charge at <https://pubs.acs.org/doi/10.1021/acsomega.3c06619>.

$^1\text{H}$  and  $^{13}\text{C}$  NMR spectra for all compounds, and raw data for MTT assays, and *in silico* predictions on the pharmacokinetics and druglikeness properties of the BCE-ring-truncated deguelin derivatives (PDF)

## ■ AUTHOR INFORMATION

### Corresponding Author

Monissa C. Paderes – Institute of Chemistry, University of the Philippines Diliman, Quezon City 1101, Philippines;  
[orcid.org/0000-0002-4042-4153](https://orcid.org/0000-0002-4042-4153); Email: [mcpaderes1@up.edu.ph](mailto:mcpaderes1@up.edu.ph)

### Author

John Alfon P. Francisco – Institute of Chemistry, University of the Philippines Diliman, Quezon City 1101, Philippines

Complete contact information is available at:

<https://pubs.acs.org/doi/10.1021/acsomega.3c06619>

### Notes

The authors declare no competing financial interest.

## ■ ACKNOWLEDGMENTS

The authors extend their immense gratitude to the Department of Science and Technology–Philippine Council for Health Research and Development (DOST-PCHRD) for funding this research under the program 'Discovery and Development of Health Products Program: Synthesis and Derivatization of Disease-Specific Bioactive Hits and Lead Compounds (Phase 2)' and supporting the acquisition of the LC-HRMS equipment of the Institute of Chemistry, University of the Philippines Diliman. The authors also thank the following facilities who aided in the completion of this study: Analytical

Services Laboratory of the Institute of Chemistry, University of the Philippines Diliman, and the Mammalian Cell Culture Laboratory of the Institute of Biology, University of the Philippines Diliman.

## REFERENCES

- (1) Takashima, J.; Chiba, N.; Yoneda, K.; Ohsaki, A. Derrisin, a New Rotenoid from *Derris malaccensis* Plain and Anti-Helicobacter pylori Activity of Its Related Constituents. *J. Nat. Prod.* **2002**, *65* (4), 611–613.
- (2) Zhang, P.; Zhang, M.; Mellich, T. A.; Pearson, B. J.; Chen, J.; Zhang, Z. Variation in Rotenone and Deguelin Contents among Strains across Four Tephrosia Species and Their Activities against Aphids and Whiteflies. *Toxins* **2022**, *14* (5), No. 339.
- (3) (a) PK, P. K.; Priyadharshini, A.; Muthukumaran, S. A Review on Rotenoids: Purification, Characterization and its Biological Applications. *Mini Rev. Med. Chem.* **2021**, *21* (13), 1734–1746. (b) Estrella-Parra, E.; Ma, C.; Gomez-Verjan, J.; González-Sánchez, I.; Vázquez-Martínez, E.; Paez-Franco, J. C.; Reyes-Chilpa, R. Rotenoids as Anticancer Agents. In *Bioactive Phytochemicals: Perspectives for Modern Medicine*; Daya-Publishing Group, 2015; Vol. 3, pp 235–258. (c) Li, L.; Wang, H.-K.; Chang, J.-J.; McPhail, A. T.; McPhail, D. R.; Terada, H.; Konoshima, T.; Kokumai, M.; Kozuka, M.; Estes, J. R.; Lee, K. H. Antitumor Agents, 138. Rotenoids and Isoflavones as Cytotoxic Constituents from *Amorpha fruticosa*. *J. Nat. Prod.* **1993**, *56* (5), 690–698.
- (4) Wang, Y.; Ma, W.; Zheng, W. Deguelin, a novel anti-tumorigenic agent targeting apoptosis, cell cycle arrest and anti-angiogenesis for cancer chemoprevention. *Mol. Clin. Oncol.* **2013**, *1* (2), 215–219.
- (5) Ferraro, M.; D'Annessa, I.; Moroni, E.; Morra, G.; Paladino, A.; Rinaldi, S.; Compostella, F.; Colombo, G. Allosteric Modulators of HSP90 and HSP70: Dynamics Meets Function through Structure-Based Drug Design. *J. Med. Chem.* **2019**, *62* (1), 60–87.
- (6) (a) Oh, S. H.; Woo, J. K.; Jin, Q.; Kang, H. J.; Jeong, J. W.; Kim, K. W.; Hong, W. K.; Lee, H. Y. Identification of novel antiangiogenic anticancer activities of deguelin targeting hypoxia-inducible factor-1 alpha. *Int. J. Cancer* **2008**, *122* (1), 5–14. (b) Oh, S. H.; Woo, J. K.; Yazici, Y. D.; Myers, J. N.; Kim, W. Y.; Jin, Q.; Hong, S. S.; Park, H. J.; Suh, Y. G.; Kim, K. W.; et al. Structural basis for depletion of heat shock protein 90 client proteins by deguelin. *J. Natl. Cancer Inst.* **2007**, *99* (12), 949–961. (c) Chun, K. H.; Kosmeder, J. W., 2nd; Sun, S.; Pezzuto, J. M.; Lotan, R.; Hong, W. K.; Lee, H. Y. Effects of deguelin on the phosphatidylinositol 3-kinase/Akt pathway and apoptosis in premalignant human bronchial epithelial cells. *J. Natl. Cancer Inst.* **2003**, *95* (4), 291–302. (d) Udeani, G. O.; Gerhäuser, C.; Thomas, C. F.; Moon, R. C.; Kosmeder, J. W.; Kinghorn, A. D.; Moriarty, R. M.; Pezzuto, J. M. Cancer chemopreventive activity mediated by deguelin, a naturally occurring rotenoid. *Cancer Res.* **1997**, *57* (16), 3424–3428.
- (7) (a) Naguib, A.; Mathew, G.; Reczek, C. R.; Watrud, K.; Ambrico, A.; Herzka, T.; Salas, I. C.; Lee, M. F.; El-Amine, N.; Zheng, W.; et al. Mitochondrial Complex I Inhibitors Expose a Vulnerability for Selective Killing of Pten-Null Cells. *Cell Rep.* **2018**, *23* (1), 58–67. (b) Liu, Y.-P.; Lee, J.-J.; Lai, T.-C.; Lee, C.-H.; Hsiao, Y.-W.; Chen, P.-S.; Liu, W.-T.; Hong, C.-Y.; Lin, S.-K.; Ping Kuo, M.-Y.; et al. Suppressive function of low-dose deguelin on the invasion of oral cancer cells by downregulating tumor necrosis factor alpha-induced nuclear factor-kappa B signaling. *Head Neck* **2016**, *38* (S1), E524–E534. (c) Dell'Eva, R.; Ambrosini, C.; Minghelli, S.; Noonan, D. M.; Albin, A.; Ferrari, N. The Akt inhibitor deguelin, is an angiopreventive agent also acting on the NF- $\kappa$ B pathway. *Carcinogenesis* **2006**, *28* (2), 404–413. (d) Lee, H.-Y.; Suh, Y.-A.; Kosmeder, J. W.; Pezzuto, J. M.; Hong, W. K.; Kurie, J. M. Deguelin-Induced Inhibition of Cyclooxygenase-2 Expression in Human Bronchial Epithelial Cells. *Clin. Cancer Res.* **2004**, *10* (3), 1074–1079. (e) Gerhäuser, C.; Mar, W.; Lee, S. K.; Suh, N.; Luo, Y.; Kosmeder, J.; Luyengi, L.; Fong, H. H. S.; Kinghorn, A. D.; Moriarty, R. M.; et al. Rotenoids mediate potent cancer chemopreventive activity through transcriptional regulation of ornithine decarboxylase. *Nat. Med.* **1995**, *1* (3), 260–266.
- (8) Caboni, P.; Sherer, T. B.; Zhang, N.; Taylor, G.; Na, H. M.; Greenamyre, J. T.; Casida, J. E. Rotenone, Deguelin, Their Metabolites, and the Rat Model of Parkinson's Disease. *Chem. Res. Toxicol.* **2004**, *17* (11), 1540–1548.
- (9) (a) Kim, W.-Y.; Chang, D. J.; Hennessy, B.; Kang, H. J.; Yoo, J.; Han, S.-H.; Kim, Y.-S.; Park, H.-J.; Geo, S.-Y.; Mills, G.; et al. A Novel Derivative of the Natural Agent Deguelin for Cancer Chemoprevention and Therapy. *Cancer Prev. Res.* **2008**, *1* (7), 577–587. (b) Chang, D.-J.; An, H.; Kim, K.-s.; Kim, H. H.; Jung, J.; Lee, J. M.; Kim, N.-J.; Han, Y. T.; Yun, H.; Lee, S.; et al. Design, Synthesis, and Biological Evaluation of Novel Deguelin-Based Heat Shock Protein 90 (HSP90) Inhibitors Targeting Proliferation and Angiogenesis. *J. Med. Chem.* **2012**, *55* (24), 10863–10884.
- (10) Garcia, J.; Barluenga, S.; Gorska, K.; Sasse, F.; Winssinger, N. Synthesis of deguelin-biotin conjugates and investigation into deguelin's interactions. *Bioorg. Med. Chem.* **2012**, *20* (2), 672–680.
- (11) (a) Liu, B.; Wu, Y.; Qin, D.; Wang, H.; Chen, H.; Zhang, Y.; Xiao, W.; Li, X.; Wang, R.; Zhang, R. Discovery of deguelin derivatives in combination with fluconazole against drug-resistant *Candida albicans*. *Med. Chem. Res.* **2023**, *32*, 2196–2207, DOI: 10.1007/s00044-023-03118-7. (b) Lokhande, K. B.; Ghosh, P.; Nagar, S.; Swamy, K. V. Novel B, C-ring truncated deguelin derivatives reveals as potential inhibitors of cyclin D1 and cyclin E using molecular docking and molecular dynamic simulation. *Mol. Diversity* **2022**, *26* (4), 2295–2309. (c) Nguyen, C. T.; La, M. T.; Ann, J.; Nam, G.; Park, H. J.; Park, J. M.; Kim, Y. J.; Kim, J. Y.; Seo, J. H.; Lee, J. Discovery of a simplified deguelin analog as an HSP90 C-terminal inhibitor for HER2-positive breast cancer. *Bioorg. Med. Chem. Lett.* **2021**, *45*, No. 128134. (d) Nguyen, C. T.; Ann, J.; Sahu, R.; Byun, W. S.; Lee, S.; Nam, G.; Park, H. J.; Park, S.; Kim, Y. J.; Kim, J. Y.; et al. Discovery of novel anti-breast cancer agents derived from deguelin as inhibitors of heat shock protein 90 (HSP90). *Bioorg. Med. Chem. Lett.* **2020**, *30* (17), No. 127374. (e) Hong, S.-J.; Kim, J.-T.; Kim, S.-J.; Cho, N.-C.; Kim, K.; Lee, S.; Suh, Y.-G.; Cho, K.-C.; Kim, K. P.; Surh, Y.-J. An Electrophilic Deguelin Analogue Inhibits STAT3 Signaling in H-Ras-Transformed Human Mammary Epithelial Cells: The Cysteine 259 Residue as a Potential Target. *Biomedicines* **2020**, *8* (10), No. 407. (f) Zhou, H.; Dong, Y.; Ma, X.; Xu, J.; Xu, S. Development of a novel truncated deguelin derivative possessing nitric oxide donor as a potential anti-lung cancer agent. *Fitoterapia* **2020**, *146*, No. 104670. (g) Kim, H. S.; Hoang, V. H.; Hong, M.; Kim, K. C.; Ann, J.; Nguyen, C. T.; Seo, J. H.; Choi, H.; Yong Kim, J.; Kim, K. W.; et al. Investigation of B,C-ring truncated deguelin derivatives as heat shock protein 90 (HSP90) inhibitors for use as anti-breast cancer agents. *Bioorg. Med. Chem.* **2019**, *27* (7), 1370–1381. (h) Yao, H.; Xu, F.; Wang, G.; Xie, S.; Li, W.; Yao, H.; Ma, C.; Zhu, Z.; Xu, J.; Xu, S. Design, synthesis, and biological evaluation of truncated deguelin derivatives as Hsp90 inhibitors. *Eur. J. Med. Chem.* **2019**, *167*, 485–498. (i) An, H.; Lee, S.; Lee, J. M.; Jo, D. H.; Kim, J.; Jeong, Y. S.; Heo, M. J.; Cho, C. S.; Choi, H.; Seo, J. H.; et al. Novel Hypoxia-Inducible Factor 1 $\alpha$  (HIF-1 $\alpha$ ) Inhibitors for Angiogenesis-Related Ocular Diseases: Discovery of a Novel Scaffold via Ring-Truncation Strategy. *J. Med. Chem.* **2018**, *61* (20), 9266–9286. (j) Lee, S. C.; Min, H. Y.; Choi, H.; Bae, S. Y.; Park, K. H.; Hyun, S. Y.; Lee, H. J.; Moon, J.; Park, S. H.; Kim, J. Y.; et al. Deguelin Analogue SH-1242 Inhibits Hsp90 Activity and Exerts Potent Anticancer Efficacy with Limited Neurotoxicity. *Cancer Res.* **2016**, *76* (3), 686–699. (k) Kim, H. S.; Hong, M.; Ann, J.; Yoon, S.; Nguyen, C. T.; Lee, S. C.; Lee, H. Y.; Suh, Y. G.; Seo, J. H.; Choi, H.; et al. Synthesis and biological evaluation of C-ring truncated deguelin derivatives as heat shock protein 90 (HSP90) inhibitors. *Bioorg. Med. Chem.* **2016**, *24* (22), 6082–6093. (l) Lee, S. C.; Min, H. Y.; Choi, H.; Kim, H. S.; Kim, K. C.; Park, S. J.; Seong, M. A.; Seo, J. H.; Park, H. J.; Suh, Y. G.; et al. Synthesis and Evaluation of a Novel Deguelin Derivative, L80, which Disrupts ATP Binding to the C-terminal Domain of Heat Shock Protein 90. *Mol. Pharmacol.* **2015**, *88* (2), 245–255. (m) Kim, H. S.; Hong, M.; Lee, S. C.; Lee, H. Y.; Suh, Y.



G.; Oh, D. C.; Seo, J. H.; Choi, H.; Kim, J. Y.; Kim, K. W.; et al. Ring-truncated deguelin derivatives as potent Hypoxia Inducible Factor-1 $\alpha$  (HIF-1 $\alpha$ ) inhibitors. *Eur. J. Med. Chem.* **2015**, *104*, 157–164.

(12) (a) Fokialakis, N.; Lambrinidis, G.; Mitsiou, D. J.; Aliogiannis, N.; Mitakou, S.; Skaltsounis, A. L.; Pratsinis, H.; Mikros, E.; Alexis, M. N. A new class of phytoestrogens; evaluation of the estrogenic activity of deoxybenzoin. *Chem. Biol.* **2004**, *11* (3), 397–406. (b) Ahmad, R.; Khan, M.; Alam, A.; Elhenawy, A. A.; Qadeer, A.; AlAsmari, A. F.; Alharbi, M.; Alasmari, F.; Ahmad, M. Synthesis, molecular structure and urease inhibitory activity of novel bis-Schiff bases of benzyl phenyl ketone: A combined theoretical and experimental approach. *Saudi Pharm. J.* **2023**, *31* (8), No. 101688.

(13) Chang, H.-H.; Ko, H.-H.; Lu, T.-M.; Lin, J.-Y.; Chang, D.-C.; Chu, T. W.; Hung, C.-F. Inhibition of UVA Damage on Human Skin Dermis Fibroblasts by the Isoflavonoid Intermediate Deoxybenzoin-3A. *Chem. Res. Toxicol.* **2021**, *34* (4), 1133–1139.

(14) (a) Li, H.-Q.; Xue, J.-Y.; Shi, L.; Gui, S.-Y.; Zhu, H.-L. Synthesis, crystal structure and antimicrobial activity of deoxybenzoin derivatives from genistein. *Eur. J. Med. Chem.* **2008**, *43* (3), 662–667. (b) Li, H.-Q.; Xiao, Z.-P.; Yin, L.; Yan, T.; Lv, P.-C.; Zhu, H.-L. Amines and oximes derived from deoxybenzoin as *Helicobacter pylori* urease inhibitors. *Eur. J. Med. Chem.* **2009**, *44* (5), 2246–2251. (c) Li, H.-Q.; Luo, Y.; Lv, P.-C.; Shi, L.; Liu, C.-H.; Zhu, H.-L. Design and synthesis of novel deoxybenzoin derivatives as FabH inhibitors and anti-inflammatory agents. *Bioorg. Med. Chem. Lett.* **2010**, *20* (6), 2025–2028. (d) Goto, H.; Kumada, Y.; Ashida, H.; Yoshida, K.-i. Discovery of Novel 2',3',4'-Trihydroxy-2-phenylacetophenone Derivatives as Anti-Gram-Positive Antibacterial Agents. *Biosci., Biotechnol., Biochem.* **2009**, *73* (1), 124–128.

(15) Li, H.-Q.; Luo, Y.; Song, R.; Li, Z.-L.; Yan, T.; Zhu, H.-L. Design, Synthesis, and Immunosuppressive Activity of New Deoxybenzoin Derivatives. *ChemMedChem* **2010**, *5* (7), 1117–1122.

(16) Huang, J.; Zhou, Z.; Zhou, M.; Miao, M.; Li, H.; Hu, Q. Development of benzoxazole deoxybenzoin oxime and acyloxylamine derivatives targeting innate immune sensors and xanthine oxidase for treatment of gout. *Bioorg. Med. Chem.* **2018**, *26* (8), 1653–1664.

(17) Mosmann, T. Rapid colorimetric assay for cellular growth and survival: Application to proliferation and cytotoxicity assays. *J. Immunol. Methods* **1983**, *65* (1), 55–63.

(18) Daina, A.; Michielin, O.; Zoete, V. SwissADME: a free web tool to evaluate pharmacokinetics, drug-likeness and medicinal chemistry friendliness of small molecules. *Sci. Rep.* **2017**, *7* (1), No. 42717.

(19) Banerjee, P.; Eckert, A. O.; Schrey, A. K.; Preissner, R. ProTox-II: a webserver for the prediction of toxicity of chemicals. *Nucleic Acids Res.* **2018**, *46* (W1), W257–W263.

(20) (a) Zhao, H.; Vandenbossche, C. P.; Koenig, S. G.; Singh, S. P.; Bakale, R. P. An Efficient Synthesis of Enamides from Ketones. *Org. Lett.* **2008**, *10* (3), 505–507. (b) Hernandez, R. D.; Genio, F. A. F.; Casanova, J. R.; Conato, M. T.; Paderes, M. C. Antiproliferative Activities and SwissADME. *ChemistryOpen* **2023**, e202300087.

(21) Lipinski, C. A.; Lombardo, F.; Dominy, B. W.; Feeney, P. J. Experimental and computational approaches to estimate solubility and permeability in drug discovery and development settings IPII of original article: S0169–409X(96)00423–1. The article was originally published in *Advanced Drug Delivery Reviews* **23** (1997) 3–25.1. *Adv. Drug Delivery Rev.* **2001**, *46* (1), 3–26.

(22) Sangthong, S.; Krusong, K.; Ngamrojanavanich, N.; Vilaivan, T.; Puthong, S.; Chandchawan, S.; Muangsin, N. Synthesis of rotenoid derivatives with cytotoxic and topoisomerase II inhibitory activities. *Bioorg. Med. Chem. Lett.* **2011**, *21* (16), 4813–4818.

(23) Gao, F.; Yu, X.; Li, M.; Zhou, L.; Liu, W.; Li, W.; Liu, H. Deguelin suppresses non-small cell lung cancer by inhibiting EGFR signaling and promoting GSK3 $\beta$ /FBW7-mediated Mcl-1 destabilization. *Cell Death Dis.* **2020**, *11* (2), 143.